Feature Extraction of Neuronal Activity by Attractor Reconstruction in Neural Networks with Delayed Couplings

Yoko Uwate†, Marie Engelene J. Obien‡, Urs Frey‡ and Yoshifumi Nishio†
† Dept. of Electrical and Electronic Engineering, Tokushima University
2-1 Minami-Josanjima, Tokushima, Japan
Email: {uwate, nishio}@ee.tokushima-u.ac.jp
‡ MaxWell Biosystems
Albisriederstrasse 253, 8047 Zurich, Switzerland
Email: {marie.obien, urs.frey}@mxwbio.com

2024 IEEE International Symposium on Circuits and Systems (ISCAS) | 979-8-3503-3099-1/24/$31.00 ©2024 IEEE | DOI: 10.1109/ISCAS58744.2024.10557836

***Abstract*—We investigate neural activity of the neural network including delayed couplings by using attractor reconstruction images. The paper presents the effects on neural activity when the value and distribution of delayed coupling is changed. In particular, we focus on the complexity of attractor images and evaluate the relationship between delayed coupling and complexity.**

I. Introduction

In the field of neuroscience, several types of neuronal activity measurement devices equipped with high-density electrode array have been developed [1]- [3]. With the development of these technologies, it has become possible to obtain more accurate data on neural activity in brains of Wistar rats and other animals [4]. Typically, neural activity data from the brain is obtained in the form of a raster plot, a graph that represents the activity patterns of neurons. Standard analysis methods include focusing on areas where many neurons are spiking simultaneously, calculating the synchronization rate of spikes, and investigating the distribution between spikes [5]. These analytical methods are important for evaluating the state of neural activity in the brain.

There have been many investigations of neural activity in networks using mathematical models as a modeling of brain network function. In Ref. [6], the authors have reported that the interaction of delay and STDP causes spiking neurons to spontaneously self-organize into groups, generating a pattern of canonical polysynchronous activity. Another study investigated the relationship between neuronal synchronization and excitatory and inhibitory conduction in a neuronal network consisting of adaptive integrating firing neurons [7].

As a feature extraction and visualization of neuronal activity, a method that converts raster plots obtained from Wistar rat brain to time series data and using attractor reconstraction has been proposed [8]. In addition, it has been shown that attractor reconstruction can also be used for neuronal activity obtained from the coupled system of the Izikevich neuronal model to characterize the network [9], [10]. The analysis methods for neural activity patterns so far have mostly been linear, however the proposed approach here is a new attempt using nonlinear methods. Since neural activity patterns exhibit highly complex features, it is believed that non-linear analysis is effective.

In this study, we investigate how attractor reconstruction is affected when delayed coupling is added to the Izikevich neuron coupling system. By using the computer simulations, we found that the pattern of neuronal activity changes with the size and distribution of the delayed couplings. In particular, the variety of delayed couplings is important for the complexity of neuronal activity.

II. Neuron and Network Models

The Izikevich neuron model which is described by a second-order differential equation Eq. (1) is used.

$$\begin{cases} \dot{v} = 0.04v^2 + 5v + 140 - u + I_{ex} \\ \dot{u} = a(bv - u) \end{cases} \tag{1}$$

if $v > 30$ mV, then $v \leftarrow c$ and $u \leftarrow u + d$.

Where v corresponds the membrane potential of the neuron, u corresponds a slow membrane recovery variable, accounting for the activation of K^+ ion currents and inactivation of Na^+ ion currents. I_{ex} denotes the excitatory input current. The parameters of the excitatory neurons (Regular Spike type) are fixed with a=0.02, b=0.2, c=-55 and d=8. The parameters of the inhibitory neurons (Frast Spike type) are fixed with a=0.1, b=0.2, c=-55 and d=2. In this case, 1,000 neurons are coupled randomly with coupling probability $p = 0.1$. The ratio of excitability and inhibitory neuron is 0.8 and 0.2, respectively.

III. Attractor Reconstruction

The attractor of dynamical systems can be reconstructed topologically in the embedding space from Takens' theorem [11]. The state vectors in the reconstructed m-dimensional embedding space are defined by

$$y(t) = x(t), x(t+\tau), ..., x(t+(m-1)\tau) \tag{2}$$

where $x(t)$ means a scalar time series and τ is the delay time.

IV. Simulation Results

A. Without Delayed Couplings

First, we investigate neuronal activity in the neural network without delayed couplings. Figure 1 shows the simulation results of the raster plot and spike rate during 1,000 [ms]. It was observed that the pattern of many neurons firing simultaneously at intervals of 100 to 200 [ms]. The time series of spike rates shows that the peaks appear irregularly and their peak values are not constant.

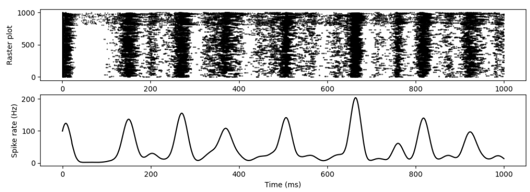

Fig. 1. Raster plot and spike rate without delayed couplings.

Action potentials of three randomly selected neurons are shown in Fig. 2. Two neurons behave in regular spikes, however one neuron produces bursting at some intervals.

The attractor obtained by applying the attractor reconstruction to the spike rate time series is shown in Fig. 3. The attractor trajectories are not random, but have a certain structure and complexity for small values.

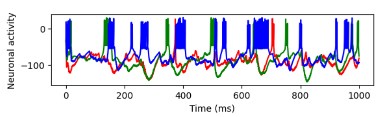

Fig. 2. Examples of three neuronal activities without delayed couplings.

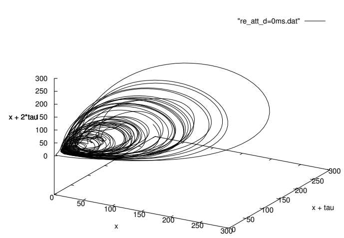

Fig. 3. Reconstracted attractor without delayed couplings (τ=10).

B. Constant Delayed Couplings

Simulation results for the case all excitatory coupling delays were set to the same value are shown in Figs. 4 and 5. In this case, all delays of inhibitory coupling were fixed at 3 [ms].

When the delay is 1 [ms], Fig. 4(a) shows that the percentage of neurons that fire simultaneously is large. And the interval of their firing timing is longer than when there is no delay. The action potentials of the neurons show that the three neurons are nearly synchronized (Fig. 5(a)). While, the case of delay is 5 [ms], Fig. 4(b) shows that the percentage of neurons that fire simultaneously is small. Three neurons are not synchronized as shown in Fig. 5(b). As the delay time becomes even longer, the spike timing becomes more periodic (Fig. 4(c) and (d)). Neuron activities are also nearly synchronous as shown in Figs. 5 (c) and (d).

Figure 6 shows the reconstructed attractors depending on the delay time. When the delay is 1 [ms], the shape of the attractor is similar to that without delay. The size of the attractor increases, and the complexity seems to be slightly weaker. When the delay is 5 ms, the attractor size is smaller and the complexity is stronger. If the delay is 10 or 12 [ms], the attractor orbit becomes nearly periodic. The size of the attractor is larger with a delay of 12 [ms]. In other words, many neurons fire at the same time.

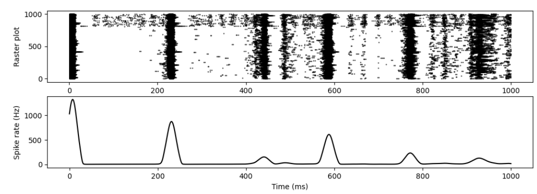

(a) Delay time: 1 [ms].

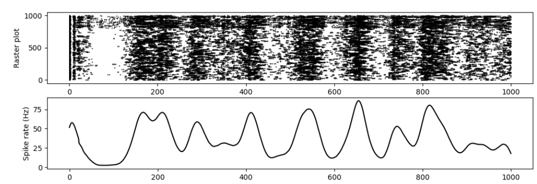

(b) Delay time: 5 [ms].

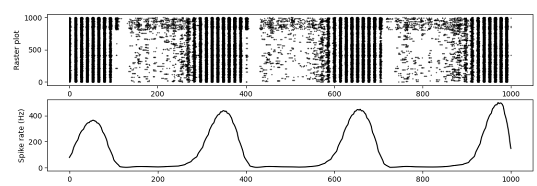

(c) Delay time: 10 [ms].

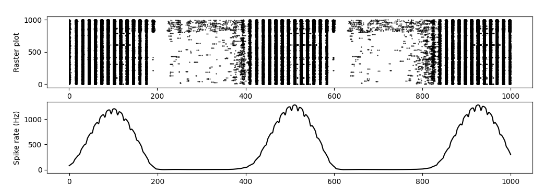

(d) Delay time: 12 [ms].

Fig. 4. Raster plot and spike rate with constant delayed couplings.

Figure 7 shows the average spike rates when the delayed coupling time is changed from 0 to 13 [ms]. This result is the average of 10 different networks with different coupling patterns. The average spike rate is larger once when there is a 1 [ms] delay than without delay, however the average spike rate becomes smaller when the delay is longer than 2 [ms].

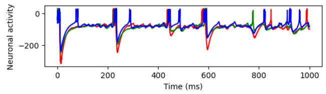

(a) Delay time: 1 [ms].

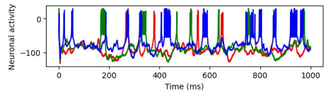

(b) Delay time: 5 [ms].

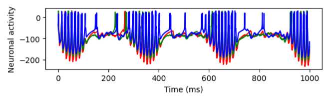

(c) Delay time: 10 [ms].

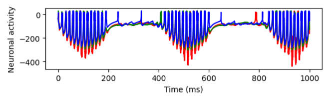

(d) Delay time: 12 [ms].

Fig. 5. Examples of three neuronal activities with constant delayed couplings.

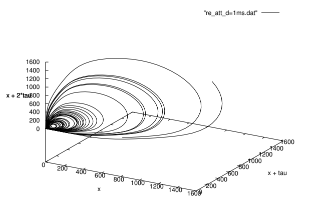

(a) Delay time: 1 [ms].

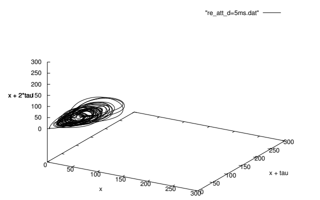

(b) Delay time: 5 [ms].

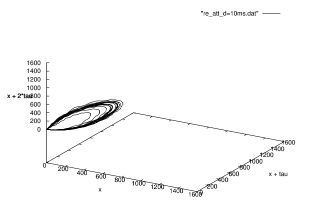

(c) Delay time: 10 [ms].

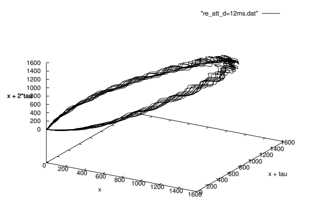

(d) Delay time: 12 [ms].

Fig. 6. Reconstracted attractors with constant delay couplings.

Then, when the delay is more than 9 [ms], the average spike rate is again larger than without delay. This may be due to an increase in the proportion of synchronous neurons as the delay time becomes longer.

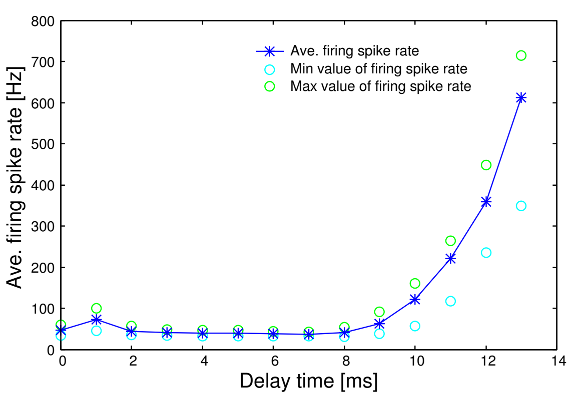

Fig. 7. Average of spike rate without delay couplings.

C. Distributed Delayed Couplings

Next, we investigate the case of four distributions of delyed couplings. Four distributions is shown in Fig. 8. The horizontal axis represents the time delay and the vertical axis represents the number of couplings. Distribution A is a uniform distribution. Distribution B is a normal distribution. Distribution C is a distribution with many couplings of short and long delays. Distribution D has the highest number of couplings for short delays, and the number of couplings decreases for longer delays.

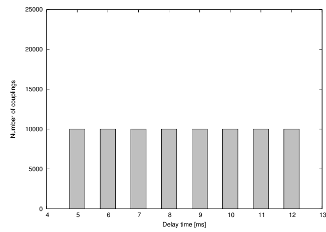

(a) Distribution A.

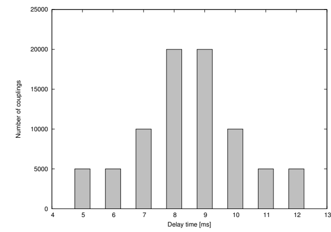

(b) Distribution B.

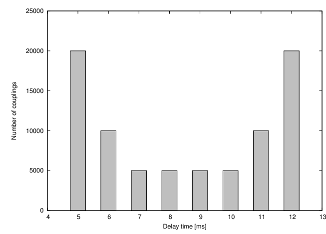

(c) Distribution C.

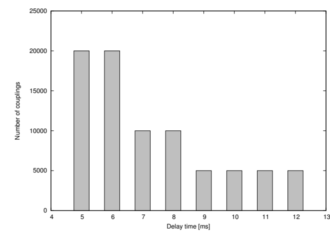

(d) Distribution D.

Fig. 8. Four patterns of distributed delayed couplings.

The simulation results of raster plot and spike rate depending on the coupling distributions are shown in Figs. 9. In the case of Distribution A, the spike firing peaks are observed at intervals of about 200 [ms]. In the case of Distribution B, similar to A, spike firing peaks are observed at about 200 [ms] intervals, and occasionally the spike rate peaks are high. In cases C and D, the peak period of spike rates is broken compared to the case without delay.

Figure 10 shows the neuronal activities of three neurons selected randamly. In all cases, we see that there are regular and burst spiking neurons.

Figure 11 shows the reconstructed attractors depending on the delay distributions. It can be seen that case of Distribution B has the largest attractor size. In all other cases, the attractor size is about the same. With regarding complexity, the complexity is stronger in cases Distributions A, C, and D compared to without delay, and it is weaker in case of Distribution B.

The average spike rate with four different distributed delayed couplings are summarized in Table I. This result is the average of 10 different networks with different coupling patterns. It can be seen that the delayed coupling reduces the mean spike rates for all distributions compared to without delay case.

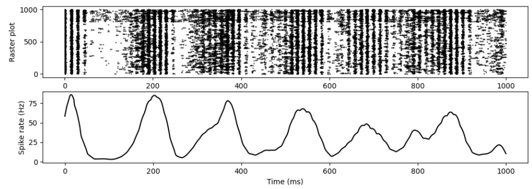

(a) Distribution A.

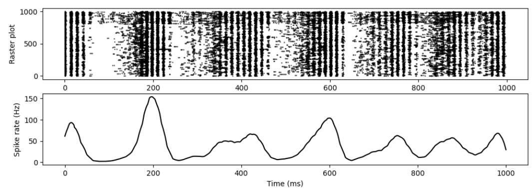

(b) Distribution B.

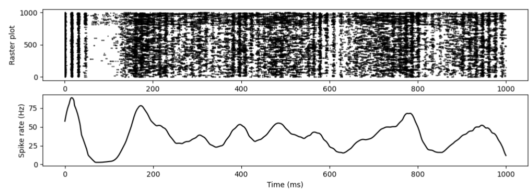

(c) Distribution C.

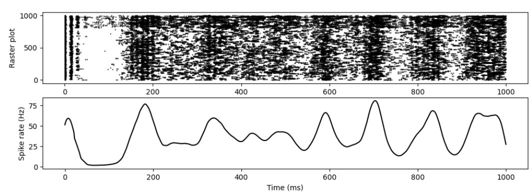

(d) Distribution D.

Fig. 9. Raster plot and spike rate with distributed delayed couplings.

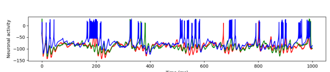

(a) Distribution A.

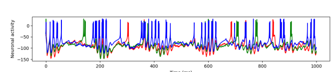

(b) Distribution B.

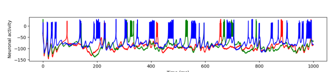

(c) Distribution C.

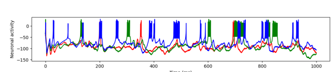

(d) Distribution D.

Fig. 10. Examples of three neuronal activities with distributed delayed couplings.

TABLE I
AVERAGE SPIKE RATE WITH DISTRIBUTED DELAY COUPLINGS

Distribution type	Ave.	Min	Max
A	35.80	30.77	40.77
B	37.83	30.12	46.90
C	36.14	31.21	40.15
D	38.55	31.90	44.05
Without Delay	46.97	35.05	60.41

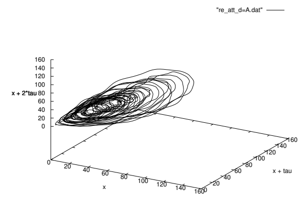

(a) Distribution A.

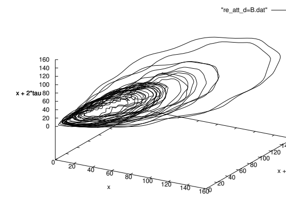

(b) Distribution B.

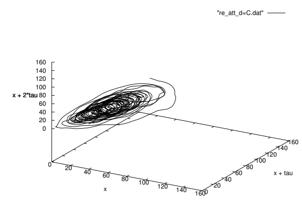

(c) Distribution C.

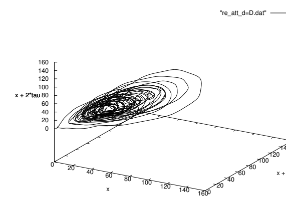

(d) Distribution D.

Fig. 11. Reconstracted attractors with distributed delay couplings.

V. CONCLUSION

We investigated how delayed coupling affects the activity patterns of neurons using images of reconstructed attractors. We showed the simulation results of raster plot, spike rate and neuronal activities. Then we apply attractor reconstruction method to spike rate time series. In particular, the evaluation focused on attractor size and complexity compared to without delay. First, in the case of that delay is constant, the attractor size becomes larger when delay time is 1 [ms]. The complexity of attractor becomes stronger when delay time is 5 [ms]. The complexity becomes weak when the delay time is longer than 10 [ms]. Next, in the case of the four distributed delayed coupling, attractor size became smaller in all cases. In complexity, we found that complexity holds in all three cases except for the normal distribution. These findings indicate that delayed coupling has a significant effect on neuronal activity. We also confirmed that the diversity of delayed couplings is important for maintaining complexity.

As the part of future work, complexity must first be quantitatively evaluated. One possible way is that we use Poincare cross sections. Also, since we did not focus on synchronization of neurons in this study, the effect of delayed coupling on synchronization should be investigated. Furthermore, while this study applied nonlinear analysis to the neural activity patterns of mathematical models, in the future, we aim to extract new features from actual neuron signals from a nonlinear perspective.

REFERENCES

[1] U. Frey, J. Sedivy, F. Heer, R. Pedron, M. Ballini, J. Mueller, A. Hierlemann, "Switch-Matrix-Based High- Density Microelectrode Array in CMOS Technology," IEEE Journal of Solid-State Circuits, 45(2), 467482. 2010.

[2] J. Muller, M. Ballini, P. Livi, Y. Chen, M. Radivojevic, A. Shadmani, V. Viswam, I. L. Jones, M. Fiscella, R. Diggelmann, Alexander Stettler, U. Frey, D. J. Bakkum and A. Hierlemanna, "High-resolution CMOS

MEA Platform to Study Neurons at Subcellular, Cellular, and Network Levels," Lab Chip 15, 2767-2780, https://doi.org/10.1039/C5LC00133A, 2015.

[3] H. Shin, S. Jeong, J. H. Lee, W. Sun, N. Choi and I. J. Cho, "3D High-Density Microelectrode Array with Optical Stimulation and Drug delivery for Investigating Neural Circuit Dynamics," Nature Communications, vol. 12, Article number: 492, 2021.

[4] D. J. Bakkum U. Frey, M. Radivojevic, T. L. Russell, J. Mller, M. Fiscella, A. Hierlemann, "Tracking Axonal Action Potential Propagation on a High-Density Microelectrode Array Across Hun- dreds of Sites," Nature Communications, 4, 2181. http://doi.org/10.1038/ncomms3181, 2013.

[5] D. J. Bakkum, M. Radivojevic, U. Frey, F. Franke, A. Hierlemann and H. Takahashi, "Parameters for burst detection," iFront. Comput. Neurosci., https://doi.org/10.3389/fncom.2013.00193, 13 January 2014.

[6] E. M. Izhikevich , "Polychronization: computation with spikes," Neural Comput. 18(2):245-82 Feb. 2006.

[7] P. R. Protachevicz, F. S. Borges, K. C. Iarosz, M. S. Baptista, E. L. Lameu, M. Hansen, I, L. Caldas, J. D. Szezech Jr., A. M. Batista, J. Kurths, "Influence of Delayed Conductance on Neuronal Synchronization," Front. Physiol., 3, https://doi.org/10.3389/fphys.2020.01053, Sep. 2020.

[8] Y. Uwate, M. E. J. Obien, U. Frey and Y. Nishio, "Time Series Analysis of Neurons and Visualization of Network Characteristics," Proceedings of RISP International Workshop on Nonlinear Circuits, Communications and Signal Processing (NCSP'19), pp. 450-453, Mar. 2019.

[9] Y. Uwate, Y. Nishio, M. E. J. Obien and U. Frey, "Visualization of Neuron Data Using Nonlinear Technic," Proceedings of International SoC Design Conference (ISOCC'19), pp. 142–143, Oct. 2019.

[10] Y. Uwate, Y. Nishio, M. E. J. Obien and U. Frey, "Nonlinear Time Series Analysis of Spike Data of Izhikevich Neuron Model," Proceedings of International SoC Design Conference (ISOCC'20), pp. 203–204, Oct. 2020.

[11] F. Takens, "Detecting Strange Attractors in Turbulence," In D.A. Rand and B.-S. Young, editors, Dynamical Systems and Turbulence, vol. 898 of Lecture Notes in Mathematics, pp. 366–381, Warwick 1980, 1981.